THERMAL PROPERTIES OF WATER IN MYOGLOBIN CRYSTALS AND SOLUTIONS AT SUBZERO TEMPERATURES

WOLFGANG DOSTER, ANTON BACHLEITNER, RAINER DUNAU, MANFRED HIEBL, AND EDGAR LÜSCHER

Physik-Department E13, Technische Universität München, D-8046 Garching, Federal Republic of Germany

ABSTRACT The water of hydration in myoglobin crystals and solutions was studied at subzero temperatures by calorimetry and infrared spectroscopy (ir). For comparison we also investigated glycine, DL-alanine and DL-valine solutions. The hydration water remains amorphorus at low temperatures. We find a broad glass transition between 180 and 270 K depending on the degree of hydration. The ice component shows a noncolligative melting point depression that is attributed to a finite conformational flexibility. The ir spectrum and the specific heat of water in myoglobin crystals was determined for the first time between 180 and 290 K. The glass transition in crystals is qualitatively similar to what is found in amorphous samples at the same water content. These data are compared with Mössbauer experiments and dielectric relaxation of water in myoglobin crystals. The similar temperature dependencies suggest a cross correlation between structural fluctuations and the thermal motion of crystal water. A hydrogen bond network model is proposed to explain these features. The essential ingredients are cooperativity and a distribution of hydrogen-bonded clusters.

INTRODUCTION

Organisms have learned to survive at subzero temperatures. Some of the mechanisms involved to avoid intracellular ice crystallization work on a molecular level. Most woody species prevent freezing in some of their tissue by deep supercooling (1). The blood of arctic fish contains antifreeze glycoproteins that inhibit freezing even in the presence of ice crystals (2, 3). It is well known that the water of hydration of proteins ($h \simeq 0.4$ g H_2O/g protein) does not crystallize at low temperatures (4). Low temperature experiments with protein solutions are required to understand the nature of supercooling and its effect on protein function. Furthermore, measurements over a wide range of temperatures help to unravel complex multistep processes occurring in proteins. Frauenfelder and coworkers (5, 6) have analyzed ligand binding to heme proteins by laser flash photolysis between 2 and 300 K. They find complex, nonexponential kinetics in contrast to exponential recombination at room temperature. It is assumed that conformational fluctuations are frozen at low temperatures leading to a distribution of binding rates. The role of the solvent in these experiments is not well understood. Freezing of conformational transitions may be related to freezing of hydration water. The x-ray structure of myoglobin (7, 8), the Lamb-Mössbauer factor of the heme iron in myoglobin crystals (9) and solutions (10) and the dielectric relaxation rate of water in myoglobin crystals (11) have been investigated at subzero temperatures. Thus myoglobin is a test case that may allow the establishment of dynamic correlations between the thermal motion of the solvent, structural fluctuations and ligand binding. Here we focus on the thermal properties of the hydration shell in myoglobin. We measured the specific heat and the O—H stretching vibration of hydration water as a function of temperature by means of differential scanning calorimetry (DSC) and infrared spectroscopy (ir). The specific heat and the strength of the hydrogen bond network are a measure of the water mobility. Partial deuteration allows us to distinguish between a crystalline and an amorphous ice phase. Most experiments were performed with myoglobin crystals and myoglobin solutions at various water concentrations between 10 and 300 K. For comparison we also investigated solutions of glycine, DL alanine, and DL valine. Special attention is given to nonequilibrium freezing and melting of water in these systems. The melting point depression of bulk ice and the effect of annealing on the amorphous component is studied.

MATERIALS AND METHODS

Sample Preparation

Sigma grade I glycine, DL-alanine, and DL-valine crystals were recrystallized several times. Sigma Type II sperm whale myoglobin (Fe^{3+}) was dialyzed against distilled water. A concentrated protein solution (15 μl, 150 mg/ml) was filled into a DSC pan and dried in a desiccator over a saturated ammonium sulfate solution (82% relative humidity). The resulting compact film had good thermal contact with the pan. The

sample was kept at constant humidity for several days. Various degrees of hydration were achieved through different saturated salt solutions or by mixing dry and humid air at different flow rates in a glove box. The water content was determined to ~1% using a dry weight method. Crystals of myoglobin (Fe^{3+}) were prepared according to the method of Perutz (12). Single crystals were used, their surface was dried on a paper to remove the ammonium sulphate solution. For the ir experiments partially deuterated myoglobin solutions (5%–20% D_2O) were dried on a CaF_2 window at constant humidity. Kinetic sorption experiments showed that ~1 wk was sufficient to achieve equilibrium.

Calorimetry

The DSC was performed with a Perkin-Elmer (model DSC1B; Norwalk, CT). The instrument was calibrated with known amounts of water and saphire. The accuracy of the temperature is 0.3 K. The noise level of the DSC scans was usually ~0.01 mcal/s. The enthalpy of mixing was estimated in a thermally isolated cell equipped with a thermocouple. Slightly hydrated protein (volume fraction of the protein $\phi_2 = V_2/V = 0.65$) was mixed with water after temperature equilibration using a syringe. The final ϕ_2 was 0.57. ϕ_2 is calculated using the specific volume of myoglobin (0.74 cm^3/g) and the density of water of 20°C.

Infrared Spectroscopy

The ir spectra were recorded using a McPherson monochromator (218; McPherson, Acton, MA) and an indium antimonide detector. The resolution (between 3 and 5 cm^{-1}) was kept low to increase the transmitted intensity. Resolution was not crucial in these experiments because of the broad water bands. The ir beam was chopped at 500 Hz. The resulting signal was measured using a lock-in amplifier to enhance the signal-to-noise ratio. The optical cell was equipped with CaF_2 windows and was attached to an Oxford helium flow cryostat.

RESULTS AND DISCUSSION

Melting Point Depression of Ice in Myoglobin and Amino Acid Solutions

Fig. 1 shows DSC power-time curves of myoglobin solutions at various protein volume fractions ϕ_2. The melting peak of water is asymmetric. Similar results were obtained with collagen and DNA solutions (13, 14). The low temperature tail is nearly independent of the water content below $\phi_2 \simeq 0.62$ ($h = 0.45$ g H_2O/g protein) at constant protein mass. The peak of the melting curve decreases and shifts to lower temperatures with decreasing water content. These observations indicate the presence of two types of water: a bulk component (component I) and a protein related fraction (component II). We have analyzed the heats of fusion of component I by subtracting the contribution of component II at $\phi_2 = 0.62$. We find $h = 0.39$ g H_2O/g protein of noncrystalline water at low temperatures. Similar numbers were obtained with other techniques (15). The melting point depression ΔT_m derived from the maxima of the melting curve is shown in Fig. 2 as a function of ϕ_2. The drastic increase of ΔT_m above $\phi_2 = 0.62$ reflects the behavior of component II. Similar experiments were performed with glycine solutions. Component II is absent in this system. The melting point depression is also shown in Fig. 2. ΔT_m and the activity of the solvent a_1 in a two component solution are related by Raoult's law.

$$\frac{\Delta T_m}{T_m} = -\frac{RT_m^\circ}{\Delta H_m^\circ} \ln a_1. \qquad (1)$$

T_m° and ΔH_m° are the melting temperature and the heat of fusion of the pure solvent, respectively. a_1 can be replaced by the mole fraction x_1 if the solution is ideal. The glycine solution is ideal up to the solubility limit ($\phi_2 \sim 0.1$). ΔT_m of the myoglobin solution is small ($\phi_2 < 0.6$) but still a factor of 100 larger than what is expected for the ideal case. Polymer solutions in general are not ideal even if the heat of mixing is small. The flexibility of the polymer chain leads to an excess entropy of mixing. Flory and Huggins calculated this term in a mean field approximation (16, 17). The polymer chains were represented as random walks on a lattice, each lattice site being either occupied by one monomer or by a solvent molecule. The free energy of

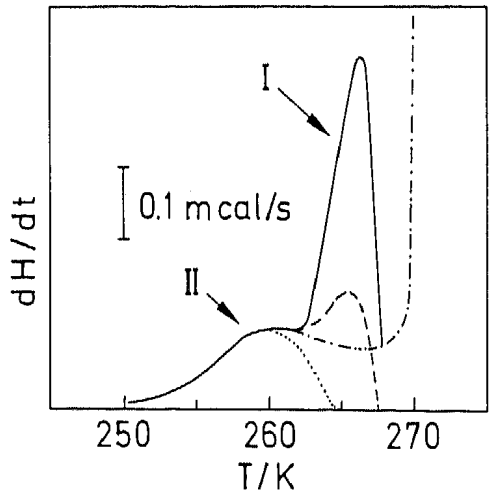

FIGURE 1 DSC power-time curves (4 deg/min) of myoglobin solutions at various protein volume fractions ϕ_2: (---) $\phi_2 = 0.35$, (—) 0.5, (---) 0.59, (· · ·) 0.63.

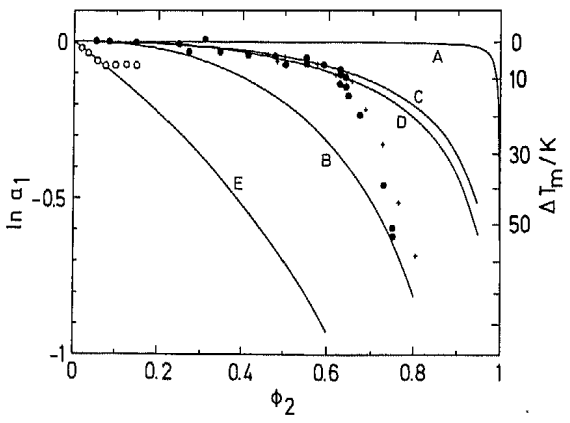

FIGURE 2 Melting point depression of water in glycine (0) myoglobin (·), and collagen solutions (+) (13) as a function of the protein volume fraction ϕ_2. Theoretical curves for $\ln a_1$ were derived from Eqs. 1, 2, and 4: (*A*) ideal myoglobin solution: Eqs. 1, $a_1 = x_1$. (*B*) Flory/Huggins model for an ideally flexible chain, Eq. 2, $\mu = 0$, $\sigma = 720$ (myoglobin). (*C*, *D*) Modified Flory/Huggins model assuming partial flexibility: Eq. 4, $\mu \sim -0.05$, for *C*, $\sigma'/\sigma = 0.25$, for *D*, $\sigma'/\sigma = 0.3$, $\sigma = 720$. (*E*) Ideal solution of separated segments: Eq. 1, $a_1 = x_1\,\phi_2$ was calculated from x_1 using the specific volumes of myoglobin $V_2 = 0.74$ cm^3/g and alanine $V_2 = 0.68$ cm^3/g.

this model has two components: an entropy term describing how many arrangements of chains can exist on the lattice for a given ϕ_2, and an energy term describing the interactions between adjacent molecules ($\sim\phi_2^2$. The solvent activity a_1 is then given by

$$\ln a_1 = \ln (1 - \phi_2) + \left(1 - \frac{1}{\sigma}\right)\phi_2 + \mu\,\phi_2^2. \tag{2}$$

σ denotes the number of chain segments of the polymer and μ is the Flory interaction parameter. μ is positive if the solvent is poor. The utility of the Flory-Huggins model for proteins is discussed in the classical paper of Kuntz and Kauzmann (4). They conclude that protein water systems appear similar to many polymer solutions. Solutions theories are more appropriate than surface theories at high and moderately high water concentrations (4). We can fit the myoglobin data using Eqs. 1 and 2 below $\phi_2 = 0.6$ with a concentration independent $\mu = 0.6$. This number, however, is not consistent with stability arguments: Eq. 2 predicts demixing at critical values of ϕ_2 and μ (18):

$$\phi_2^c = \frac{1}{\sqrt{\sigma}}$$

$$\mu^c = 0.5 + \frac{1}{\sqrt{\sigma}}. \tag{3}$$

The ratio of molecular volumes σ of myoglobin and water is 720. The critical concentration is then 50 mg/ml and $\mu^c \simeq 0.5$. Myoglobin, however, is easily soluble at higher concentrations. Thus $\mu < 0.5$ in contrast to the experimental result. μ in general contains enthalpic and entropic corrections. We have measured the enthalpic contribution by mixing water and slightly hydrated protein at equal temperatures. The final ϕ_2 was 0.57. We obtain an increase in temperature by 1.1 K, which yields μ is approximately equal to -0.05 if the specific heat of the sample is taken into account. A positive heat of mixing (negative μ) is common for polar solutes like proteins (4). The experimental value of $|\mu|$ is about a factor of 10 smaller than what is required to explain the deviation from an ideal solution based on enthalpic effects alone. We conclude that the large and positive apparent μ obtained by the fits must be an entropic correction. Consequently, this contribution is not accurately represented by an interaction term proportional to ϕ_2^2. One has to keep in mind that the Flory/Huggins model is based on the assumption of an ideally flexible polymer chain. Globular proteins, however, have a compact structure and are not ideally flexible. Only a fraction of the residues is accessible to the solvent (19). The simplest modification of the Flory/Huggins model is the assumption of partial flexibility. We expect that the average number of flexible segments is smaller than the total number of segments. This modification, already considered by Flory (16), removes the inconsistencies and yields the following solvent activity:

$$\ln a_1 = \frac{\sigma'}{\sigma}\ln (1 - \phi_2) + \left(\frac{\sigma'}{\sigma} - \frac{1}{\sigma}\right)\phi_2 + \mu\,\phi_2^2$$

$$\phi_2^c \cong \sigma'^{-0.5}, \quad \mu^c \cong \frac{\sigma'}{2\sigma}. \tag{4}$$

σ'/σ denotes the fraction of flexible segments. $\sigma' \sim \sigma$ yields Eq. 2 and $\sigma' = 1$ represents the case of solute molecules without internal flexibility. The resulting activity curves are shown in Fig. 2. The best fit of the data was obtained with σ'/σ between 0.25 and 0.3 (μ is approximately equal to -0.05). According to this model only 40–50 of the 153 residues in myoglobin are flexible on the average. This result is not unreasonable in view of hydrogen exchange (20) and x-ray (7, 8) data. Myoglobin has 38 fast exchanging NH protons. X-ray diffraction shows that 44 resides have a mean square displacement >0.15 Å^2. Nearly all of them lie on the surface of the protein. The large noncolligative melting point depression of myoglobin solutions requires an explanation. The modified Flory/Huggins model can fit the data using a single parameter σ'/σ with a well defined physical meaning. It fails, however, at high protein volume fractions. The data above $\phi_2 = 0.62$ cannot be explained by assuming a concentration dependent μ. We show in the next section that component II in contrast to I depends on the history of the sample.

Glass Transition of Amorphous Solid Water in Myoglobin and Amino Acid Solutions

Fig. 1 shows that melting of component II starts near 250 K at high water concentrations. Above $\phi_2 \sim 0.62$ only component II is present. The melting peak of this fraction shifts to lower temperatures with decreasing water content (Fig. 2). We find that component II can be transformed partially into the crystalline component I upon annealing at water concentrations where both components are present. Fig. 3 displays the difference between two DSC

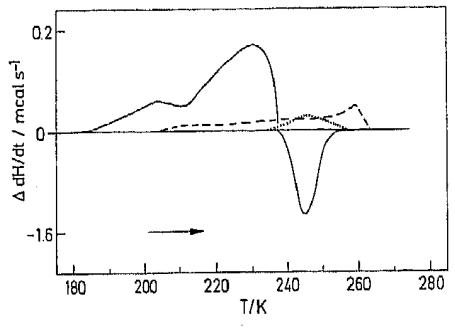

FIGURE 3 Each curve represents the difference $\Delta\, dH/dt$ between two DSC scans. The first time the sample was cooled at a fast rate while the second scan was taken after slow cooling or annealing: (—) alanine 100 mg/ml, difference plot between 10 deg/min and 1 deg/min cooling rate, (· · ·) valine 50 mg/ml, difference between 40 deg/min cooling rate and a sample annealed for 2 h at 250 K, (---) myoglobin $\phi_2 = 0.42$, difference between 20 deg/min cooling rate and annealing at 250 K for 2 h.

power-time curves at $\phi_2 = 0.42$ (broken line): In the first experiment we cooled the sample at a fast rate (40 deg/min). A DSC scan was taken. The second time the sample was cooled slowly (4 deg/min) and annealed for 2 h at 250 K. A second scan was taken after cooling to 180 K. The melting peak of this scan was less asymmetric than after fast cooling. The difference between the two scans (shown in Fig. 3) indicates a loss of component II through annealing. This result suggests that component II is amorphous solid water with a glass temperature between 250 and 260 K. We also looked for time-dependent effects in amino acid solutions with an increasing number of side chain carbons. The glycine solution did not show any transition, except the melting of bulk ice. By contrast three additional low temperature peaks were obtained with alanine solutions at cooling rates faster than 4 deg/min. Fig. 3 displays the difference between two DSC scans after fast and slow cooling (full line). The exothermic peak at 245 K indicates the freezing of water that did not have time to crystallize during the cooling cycle. This peak is constant above 10 deg/min, and is proportional to the alanine concentration. According to the heats of fusion it represents 0.7 g H_2O/g alanine. The noncrystalline water exhibits a two-step glass transition at 200 and 230 K. The peaks may result from the onset of local mobility and free diffusion of water since crystallization sets in at the end of the second transition. The rate of crystallization of hydration water in valine samples was much slower than for the alanine case. Annealing at 250 K for 2 h was necessary to obtain a difference, as shown in Fig. 3 (dotted line). A single transition near 245 K is observed. The side chain of valine has an additional carbon and is thus less soluble than alanine. The concentration was smaller by a factor of 2. These experiments show that amino acids like proteins inhibit the freezing of water. The size and the nature of the side chain has a drastic effect on the rate of crystallization. The difference between the three amino acids must be attributed to hydrophobic effects. We note that alanine is a major component of antifreeze glycoproteins (2).

Infrared Experiments with Hydrated Myoglobin Films

The ir spectrum of H_2O is complicated by the fact that the O—H stretch is coupled to other modes of motion (Fermi resonance). Therefore we partially deuterated our samples and looked at the uncoupled O—D oscillator. The ir experiments allow us to extend the DSC data to low temperatures and low water concentrations.

Fig. 4 shows the O—D stretching bands of different states of water. The absorption of water in myoglobin films at room temperature is broad with maxima at 4.049 μm (2,470 cm^{-1}) and 4.14 μm (2,415 cm^{-1}) (full line). It is redshifted relative to the spectrum of bulk water that has a maximum at 4 μm. The O—D band of bulk ice is narrow (dotted line, 40 cm^{-1}) compared to water (160 cm^{-1}). The dashed line represents the low temperature O—D spectrum of water in myoglobin films (4.175 μm). It is also shifted to higher wavelengths relative to the band of amorphous ice (dashed dotted line), which was obtained by condensation of vapor on a cold substrate (21). The redshifts indicate stronger hydrogen bonding. The half-width of the low temperature water spectrum in myoglobin films (100 cm^{-1}), is intermediate between liquid water (160 cm^{-1}) and amorphous ice (65 cm^{-1}). It strongly suggests a state in which the molecular disorder of liquid water is preserved to a large extent in spite of a drastic reduction in molecular motion. Similar conclusions were derived from other experiments (22, 23). Instead of "non-freezable" water we use "solid amorphous water" or "amorphous ice" to describe this state. Fig. 5 shows typical difference spectra at various temperatures with respect to a spectrum taken at 80 K. The figure displays the continuous transition from amorphous solid water to liquid water with increasing temperature. No change is found below 80 K. In Fig. 6 we plot the ratio of intensities at 4.175 and 4.049 μm

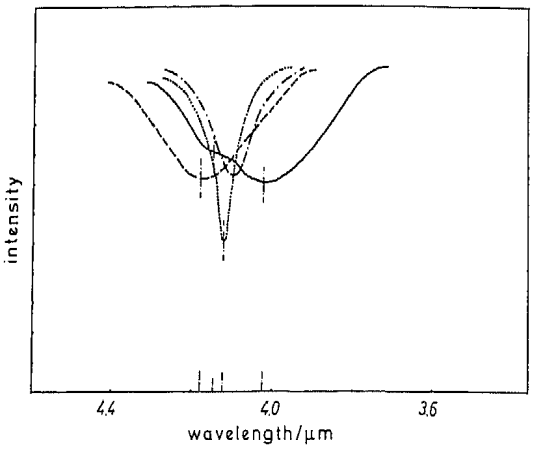

FIGURE 4 The O—D stretching absorption band of different water states (intensity in arbitrary units): (—) room temperature spectrum of myoglobin films, (· · ·) ice spectrum, (- · -) amorphous ice, (---) low temperature water spectrum in myoglobin films.

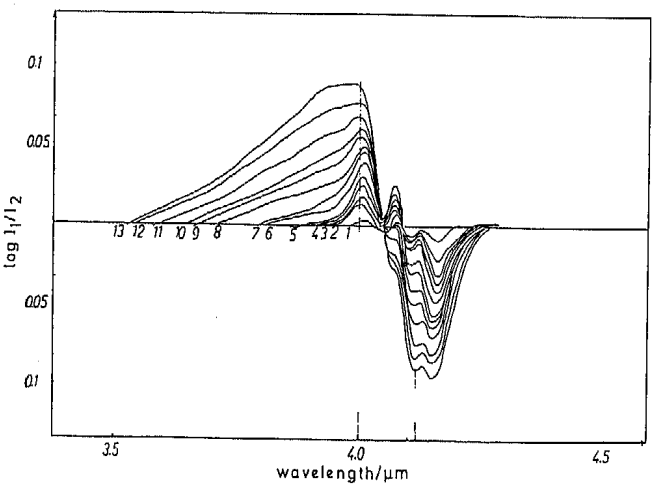

FIGURE 5 Difference spectra relative to a spectrum taken at 80 K (I_2) as a function of temperature. The hydration of this myoglobin film was 0.35 g/g protein. (1) 122 K, (2) 139 K, (3) 158 K, (4) 180 K, (5) 193 K, (6) 206 K, (7) 214 K, (8) 223 K, (9) 230 K, (10) 241 K, (11) 251 K, (12) 255 K, (13) 293 K.

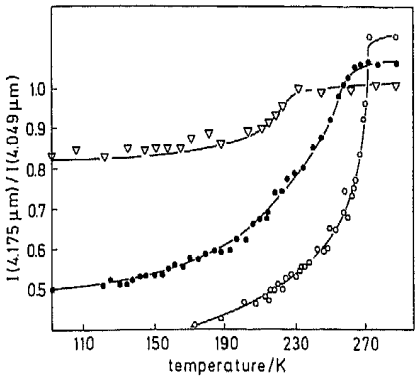

FIGURE 6 Transmitted ir intensity ratio $I(4.175)/I(4.049)$ of hydrated myoglobin films as a function of temperature. Hydration: (o) 0.46 g/g, (•) 0.37 g/g, (▽) 0.25 g/g.

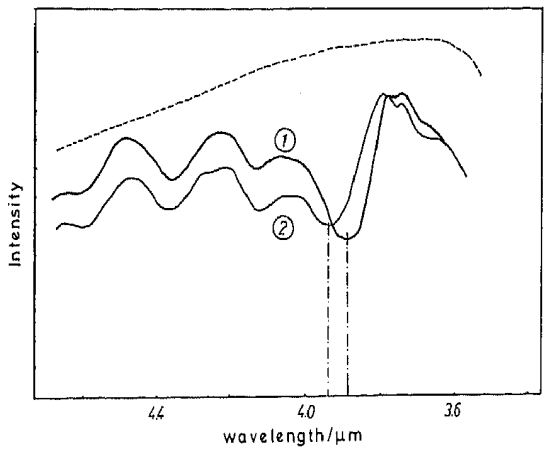

FIGURE 7 ir absorption spectrum of myoglobin crystals (O—D) at room temperature (1) and 80 K (2). The background (---) is also given on the same intensity scale.

as a function of temperature and hydration. The sample with $h = 0.46$ ($\phi_2 = 0.6$) did contain some crystalline ice. The low temperature tail is characteristic for an amorphous component and is similar to what has been found in the DSC experiments. The ir data show that this tail extends to lower temperatures than have been inferred from calorimetry. The steep rise of $I(4.175)/I(4.049)$ occurs in the temperature range where component II melts. This transition decreases in size and shifts to lower temperatures with decreasing hydration in agreement with DSC data (Fig. 2). The spectra of low humidity samples ($h \cong 0.22$) by contrast were independent of temperature between 15 and 300 K.

One can conclude that the changes of the O—D band involve water clusters and not individual molecules. This result stresses the cooperative nature of the glass transition. The cluster size determines the transition temperature and large clusters are more stable than smaller ones (Fig. 6). The heterogeneous protein surface obviously leads to a broad cluster size distribution. Amorphous solid water melts at 135 K within a few degrees (24). Amorphous ice in myoglobin solutions melts between 180 and 260 K. Stronger hydrogen bonding (Fig. 4) and the distribution of water clusters may explain these differences. We have recorded ir data of hydrated lysozyme films. The results were almost identical to the myoglobin data at the same hydration. Nuclear magnetic resonance (NMR) experiments with hydration lysozyme powder (25) support our conclusion that the hydration water is frozen below 190 K and gains mobility above this temperature.

Water in Myoglobin Crystals

DSC experiments with myoglobin crystals excluded the formation of any bulk ice. Drying the surface of single crystals on a paper to remove the solvent (a saturated ammonium sulfate solution) produced a small amount of salt crystals. These crystals exhibit a well known ferroelectric transition at 220 K (26). The transition was no longer present after washing the myoglobin crystals for a short time in ammonium phosphate solution. The specific heat of water in these crystals was determined between 180 and 270 K. The data shown in Fig. 9 (triangles) were obtained from a difference measurement relative to dried "crystals." The water has a weight fraction of 0.35 g/g protein and salt. The heat capacities of bulk ice (solid line) is also given (22). The crystal water has a glass temperature near 220 K. The transition is somewhat narrower than in amorphous samples. The specific heat approaches the ice value at the low temperature end and is slightly larger than in bulk water at high temperatures.

Fig. 7 compares the O—D spectra of crystal water at room temperature and 80 K. The room temperature band at 3.87 μm shifts to 3.95 μm at low temperatures. The peak position indicates weaker hydrogen bonding than in films. The temperature dependence of the frequency shift is displayed in Fig. 8. The spectrum is constant between 10 and 190 K. Above 190 K we observe a continuous transition similar to what is found for the specific heat (Fig. 9). Several temperature cycles were applied to insure reversibility. The temperature effects are qualitatively similar to what is obtained with amorphous samples at the same water content. The onset of water mobility in the crystals between 190 and 200 K, however, is much sharper than in the films. The average dielectric relaxation time of crystal water (11) and the Lamb-Mössbauer factor of the heme iron f_0 (17) are also shown in Fig. 8. ($-\ln f_0$) is

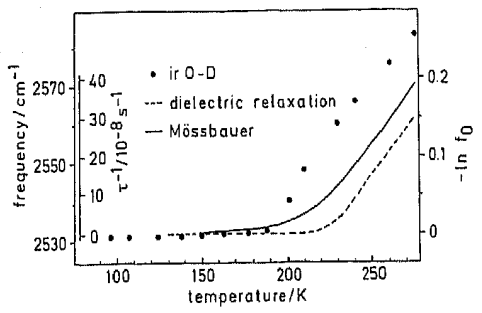

FIGURE 8 Temperature dependence of various properties of myoglobin crystals: (·) Frequency of the O—D band maximum (ir), (---) dielectric relaxation time of water (schematic) (11), (—) Lamb-Mössbauer factor f_0 after subtracting the harmonic mode (35, 36 schematic).

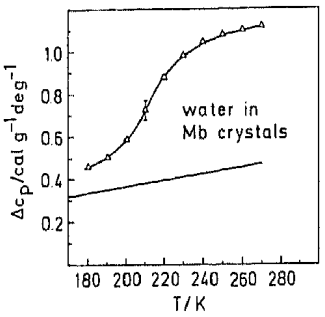

FIGURE 9 Specific heat of water in myoglobin crystals (-Δ-) as a function of temperature. The data were caluclated from the difference Δ dH/dt between two measurements. The first experiment was performed with intact crystals, the second experiment was done after drying the same crystals at 80C under nitrogen flow in the DSC apparatus. The specific heat of bulk ice (—) is also given.

proportional to the mean square displacement and thus the fluctuation intensity of the heme iron. The similarity of the temperature dependencies in Fig. 8 is striking despite unequal transition temperatures. To compare these data, it is important to account for the different experimental time scales involved. Ir spectroscopy provides an ensemble average. It yields the lowest transition temperature. The Lamb-Mössbauer factor is insensitive to motions slower than 100 ns. The dielectric experiment cannot record relaxation times that are longer than 10 ns. Therefore it is reasonable that the apparent onset of water motion in the dielectric experiment occurs at a higher temperature than what is concluded from ir spectroscopy. The ir data show that the crystal water is essentially frozen below 190 K and continuously gains mobility above this temperature. The Mössbauer data fit well into this scheme and suggest a common mechanism. Furthermore Mössbauer experiments with frozen myoglobin solutions show an additional decrease of the Lamb-Mössbauer factor above 240 K, which is absent in the crystal (10). We find that a large fraction of amorphous solid water (component II) melts above 240 K at high water concentrations. By contrast, Mössbauer experiments with dry samples yield a nearly temperature independent f_0 (28). This fact is consistent with our observations that the ir spectrum of water at low humidities is independent of temperature. All results suggest a dynamic correlation between the heme iron and the water of hydration. The same conclusion was derived from dielectric relaxation data of water in myoglobin crystals (11).

CONCLUSION

The data and the arguments given above need further inspection. A cross correlation between solvent motion and conformational fluctuations had been proposed some time ago without referring to a molecular mechanism (29, 30). A dielectric coupling between water and the protein was suggested in reference 11. The fluctuating electromagnetic field of hydration water is supposed to drive conformational motion. In our view this model needs extension, since it does not account for some essential features of the protein-water system. The solid water melts at 190 K (Fig. 8). Melting involves breaking of formation of hydrogen bonds. The protein structure, however, is stabilized by the same type of interaction. The binding energies are very similar (31). Therefore it is not surprising that mobility changes occur at similar temperatures even if protein and water were independent systems. Based on the analysis of the mean square displacement of individual atoms in lysozyme and myoglobin, Gavish (32) proposed that "some essential contributions to protein dynamics are likely to originate from the kinetics of formation and breaking of intramolecular hydrogen bonds and those resulting from protein-solvent interactions." To stress the role of the solvent we would like to add a second argument: the protein-water system is a network of hydrogen bonds. This network has no translational symmetry. It may be split into clusters with stronger internal coupling. The dynamics of these clusters involve a formation and breaking of hydrogen bonds that is predominantly a cooperative phenomenon. This view resembles the flickering-cluster model proposed by Frank (the model is discussed in reference 33) to explain the properties of liquid water. The cooperativity of the network provides the coupling mechanism between conformational motion and water fluctuations. The importance of the water cluster size can be inferred from Fig. 6: The cluster size decreases with decreasing hydration. The glass transition shifts in parallel to lower temperatures, implying that small clusters are less stable than larger ones. Consequently, the dynamics should also depend on the cluster size. On the other hand, water clusters are required to insure mobility since little motion is detected in dry proteins. Dry myoglobin can be heated at least up to 80°C without denaturation (unpublished data). It appears that a hydrogen bond can be broken only at the expense of formation of a new bond. This process is slowed if only few donors and acceptors are present. A distribution of conformational substates was invoked to explain the nonexponential ligand binding kinetics in heme proteins (5, 6). It was concluded from these experiments that each protein is frozen in a particular substate below 200 K. This distribution may reflect the distribution of hydrogen bonds that includes a multiplicity of water states on the protein surface. The redshift of the amorphous ice band by (15 20 cm^{-1}) relative to bulk ice implies an increase of the average binding energy by 3.6 kJ/mol. This shift corresponds to a shortening of the 0 ... 0 distance by 0.05 Å (34). The distribution of H-bonds may thus be inaccesible to x-ray crystallography.

Technical help and useful discussions with B. Büchner, W. Nadler, and Dr. P. Korpiun are gratefully acknowledged.

Received for publication 8 October 1985 and in final form 13 February 1986.

REFERENCES

1. George, M. F., and M. J. Burke. 1984. Supercooling of tissue water to extreme low temperatures in overwintering plants. *Trends Biochem. Sci.*. 211–214.
2. Feeney, R. E., and R. Hofmann. 1973. Depression of freezing point by glycoproteins from an antarctic fish. *Nature (Lond.)*. 243:357–358.
3. Brown, R. A., Y. Yeh, T. S. Burcham, and R. E. Feeney. 1985. Direct evidence for antifreeze glycoproteins adsorption onto an ice surface. *Biopolymers*. 24:1265–1270.
4. Kuntz, I. D., and W. Kauzmann. 1974. Hydration of proteins and polypeptides. *Adv. Protein Chem.* 28:239–345.
5. Austin, R. H., K. W. Beeson, L. Eisenstein, H. Frauenfelder, and I. C. Gunsalus. 1975. Dynamics of ligand binding to myoglobin. *Biochemistry*. 14:5355–5373.
6. Doster, W., D. Beece, S. F. Bowne, E. Di Iorio, L. Eisenstein, H. Frauenfelder, L. Reinisch, S. Shyamsunder, K. H. Winterhalter, and K. T. Yue. 1982. Control and pH dependence of ligand binding to heme proteins. *Biochemistry*. 21:4831–4839.
7. Hartmann, H., F. Parak, W. Steigemann, G. A. Petsko, D. Ringe Ponzi, and H. Frauenfelder. 1982. Conformational substates in a protein: structure and dynamics of metmyoglobin at 80 K. *Proc. Natl. Acad. Sci. USA*. 79:4967–4971.
8. Frauenfelder, H., G. A. Petsko, and D. Tsernoglou. 1979. Temperature dependent x-ray diffraction as a probe of protein structural dynamics. *Nature (Lond.)*. 280:558–563.
9. Parak, F., E. N. Frolov, R. L. Mössbauer, and V. I. Goldanskij. 1981. Dynamics of metmyoglobin crystals investigated by nuclear gamma resonance absorption. *J. Mol. Biol.* 145:825–834.
10. Keller, H., and P. G. Debrunner. 1980. Evidence for conformational and diffusional mean square displacement in frozen aqueous solution of oxymyoglobin. *Phys. Rev. Lett.* 45:68–71.
11. Singh, G. P., F. Parak, S. Hunklinger, and K. Dransfeld. 1981. Role of adsorbed water in the dynamics of metmyoglobin. *Phys. Rev. Lett.* 47:685–688.
12. Perutz, M. 1968. *J. Cryst. Growth*. 2:54–58.
13. Haly, A. R., and I. W. Snaith. 1971. Calorimetry of rat tail tendon collagen before and after denaturation: the heat of fusion of its adsorbed water. *Biopolymers*. 10:1681–1699.
14. Andronikashvili, E. L., G. M. Mrevlishvili, G. S. Japaridze, and V. M. Sokhadze. 1979. Conformational properties of biomacromolecules (proteins and nucleic acids) at low temperatures. *Int. J. Quantum Chem. Symp.* vol. XV:367–377.
15. Cantor, S., and P. Schimmel. 1980. Biophysical Chemistry. Vol II. Freeman and Company. 552.
16. Flory, P. J. 1942. Thermodynamics of high polymer solutions. *J. Chem. Phys.* 10:51–61.
17. Huggins, M. 1942. Thermodynamics properties of solutions of long-chain components. *Ann. NY Acad. Sci.* 43:1–32.
18. De Gennes, P. 1979. Incompatibility and segregation. *In* Scaling Concept in Polymer Physics. Cornell University Press, Ithaca, NY. 98–114.
19. Richards, F. 1977. Areas, volumes, packing and protein structure. *Annu. Rev. Biophys. Bioeng.* 6:151–176.
20. Englander, W. S. and N. R. Kallenbach. 1984. Hydrogen exchange and structural dynamics of proteins and nucleic acids. *Q. Rev. Biophys.* 17:521–655.
21. Nielson, G., and S. A. Rice. 1982. An improved analysis of the OH stretching spectrum of amorphous solid water. *J. Chem. Phys.* 78:4824–4827.
22. Hoeve, C. A. J., and A. S. Tata. 1978. The structure of water absorbed in collagen. *J. Phys. Chem.* 82:1660–1664.
23. Hilton, B. D., E. Hsi, and R. G. Bryant. 1977. ^{1}H nuclear magnetic resonance relaxation of water on lysozyme powders. *J. Am. Chem. Soc.* 99:8483–8490.
24. Sugisaki, M., H. Suga, and S. Seki. 1968. Calorimetric study of the glassy state: heat capacities of glassy water and cubic ice. *Bull. Chem. Soc. Jpn.* 41:2599–2603.
25. Andrew, W. R., D. J. Bryant, and T. Z. Rizvi. 1983. The role of water in the dynamics of proton relaxation of solid proteins. *Chem. Phys. Lett.* 95:463–466.
26. Hoshino, S., K. Vedam, Y. Okaya, and R. Pepinski. 1958. Dielectric and thermal study of $(NH_4)_2SO_4$ and $(NH_4)_2BeF_4$ transitions. *Phys. Rev.* 112:405.
27. Mayo, K. H., D. Kucheida, F. Parak, and J. C. W. Chien. 1983. Structural dynamics of human deoxyhemoglobin and hemochrome investigated by nuclear gamma resonances absorption. *Proc. Natl. Acad. Sci. USA*. 80:5294–5296.
28. Krupyanskii, Y. F., F. Parak, V. I. Goldanskii, R. L. Mössbauer, E. E. Gaubman, H. Engelmann, and I. P. Suzdalev. 1982. Investigation of large intramolecular movements within metmyoglobin by Raleigh scattering of Mössbauer radiation. *Z. Naturforsch.* 37c:57–62.
29. Careri, G. 1974. The fluctuating enzyme. *In* Quantum Statistical Mechanics in the Natural Sciences. Plenum Publishing Corp., New York. 15–35.
30. Careri, G., P. Fasella, and E. Gratton. 1979. Enzyme dynamics: the statistical physics approach. *Annu. Rev. Biophys. Bioeng.* 8:69–97.
31. Chotia, C. 1976. The nature of the accessible and buried surfaces in proteins. *J. Mol. Biol.* 105:1–14.
32. Gavish, B. 1983. Proteins main-chain atomic displacements and density of stabilizing interactions. *Biophys. Struct. Mech.* 10:31–45.
33. Kavanau, J. L. 1964. Water and Solute-Water Interactions. Holden-Day, Inc., Oakland, CA. 10–14.
34. Joesten, G. 1974. Hydrogen Bond. Marcel Dekker and Co.
35. Knapp, E. W., S. F. Fischer, and F. Parak. 1982. Protein dynamics from Mössbauer spectra. *J. Phys. Chem.* 86:5042–5047.
36. Nadler, W., and K. Schulten. 1984. Theory of Mössbauer spectra of proteins fluctuating between conformational substates. *Proc. Natl. Acad. Sci. USA*. 81:5719–5723.